Journal of Nepal Geological Society, 2004, Vol. 29, pp. 1-11

Numerical simulation of fault development along NE-SW Himalayan profiles in Nepal

***D. Chamlagain and D. Hayashi**

Department of Physics and Earth Sciences, University of the Ryukyus, Nishihara, Okinawa, 903-0213, Japan
*(*E-mail: dchamlagain@hotmail.com)*

ABSTRACT

We examined the state of stress in and around the Himalayan nappes via 2D finite element method using elastic rheology under plane strain condition. This paper describes how we used advanced numerical modelling technique, the finite element method to compute stress and fault as a function of rock layer properties, convergent displacement and boundary condition in the convergent tectonic environment. Interpretation of the calculated results remains somewhat ambiguous because of the limitation of elastic modelling, however, the results are still comparable with geological and geophysical data. Some interesting features of our models are: (1) compressive state of stress in Himalaya; (2) effect of geometry of MHT on stress orientation; (3) the diffuse zone of failure elements along the flat-ramp-flat regions of the Main Himalayan Thrust (MHT); (4) normal and thrust faults pattern in the vicinity of Main Boundary Thrust (MBT) and Main Frontal Thrust (MFT); (5) initiation of faults at depth and their propagation toward south under increasing convergent displacement, which is consistent with the sequence of thrusting in Himalaya; and (6) direct correlation of simulated fault patterns with geological evidences. Thus overall features of the numerical models are able to conclude that the mid-crustal ramp, MBT and MFT are the most active structures in the present day plate kinematics.

INTRODUCTION

Finite element method (FEM) is one of the useful numerical methods to simulate state of stress and resulting deformation during orogeny. The state of stress and fault development pattern are important aspects of convergent tectonic environment to understand the crustal deformation. In this regard numbers of investigations have been carried out to understand structural and tectonic evolution of the Himalayan orogenic belt. England and McKenzie (1982) carried out numerical simulation with intention to understand the deformation of the continental lithosphere in terms of the behaviour of a thin viscous sheet of material obeying a power law rheology. Similarly, Hayashi (1987) numerically simulated the uplift of the Tibetan plateau. Regarding fault development in Himalaya, Shanker et al. (2002) have successfully modelled the coeval development of the South Tibetan Detachment Fault and the Main Central Thrust using 2D elastic homogeneous wedge models. Recently, Alam and Hayashi (2003) and Howladar and Hayashi (2003) simulated stress field and fault development pattern in the Himalaya. Their models show shallow thrust faulting in Himalayan fold and thrust belt and are unable to explain deformation around mid-crustal ramp and active faults along major intracrustal thrusts.

In the present study, we use 2D elastic finite element method to investigate stress distribution and fault development pattern in and around the Himalayan nappes of Nepal Himalaya in response to boundary conditions representing accretionary prism of the fold and thrust belt under the plane strain condition. We will also focus the mode of active faulting in the Himalaya. Though our model sections cut the several nappes, the emplacement mechanism and first-order structural development of Himalayan nappes, which evolved during continued collision, are beyond the scope of this paper.

Tectonic Framework of Nepal Himalaya

The Himalaya, a typical example of a collision type orogenic belt, owes its origin to the collision between the Indian and the Eurasian continental plates, initiated in Eocene time. The convergence, deformation and uplift processes continue today with an average convergence rate of 5 cm/year (Molnar and Tapponnier 1975; Patriat and Achache 1984). The continued penetration of Indian continent under Eurasian continent produced crustal shortening and slicing of the northern margin of the Indian continent into slivers along the three major thrusts; Main Central Thrust (MCT), Main Boundary Thrust (MBT) and Main Frontal Thrust (MFT) (Thakur 2001). These thrusts are considered to join together in a decollement called the Main Himalayan Thrust (MHT) (Zhao et al. 1993). Similar to entire Himalayan range, the basic architecture of the Nepal Himalaya is controlled by these thrusts and divided into four major intracontinental thrust packages from south to north, Siwaliks, Lesser Himalayan Sequence (LHS), Higher Himalayan Sequence (HHS) and Tibetan Tethys Sequence (TTS) (Fig. 1). The Siwaliks, composed of mudstone,

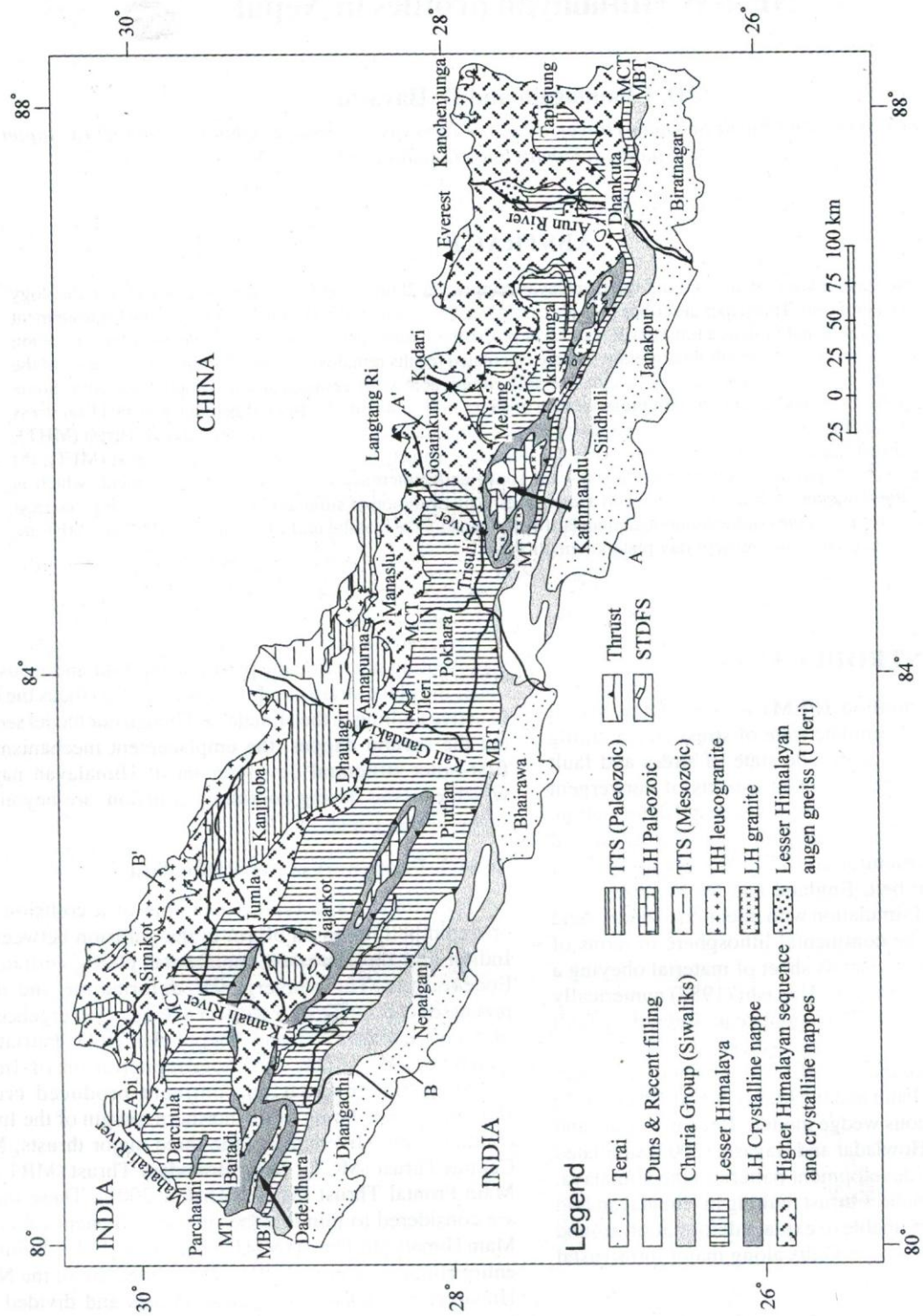

Fig. 1: Geological map of Nepal (Upreti and Le Fort, 1999). LH: Lesser Himalaya, HH: Higher Himalaya, TTS: Tibetan-Tethys sediments, MBT: Main Boundary Thrust, MCT: Main Central Thrust, MT: Mahabharat Thrust, STDS: South Tibetan Detachment System. A-A' and B-B': Cross-section lines.

sandstone and conglomerate, is bounded to the south by the active thrust fault MFT and to the north by the MBT, which brought the LHS over the Siwaliks. The LHS consisting mostly of unfossiliferous sedimentary and metasedimentary rocks, is exposed between the MBT in the south and MCT in the north. The crystalline unit of the HHS is the northern most thrust package consisting of high-grade metamorphic rocks such as gneisses, migmatites, schists, quartzites and marble. It forms basement of the overlying Tibetan-Tethys Himalaya, which is bounded by normal fault in the south (Burchfiel et al. 1992). In addition to nappes, there is an extensive, gently dipping crystalline thrust sheet in eastern Nepal, which traveled southward at least 100 km to reach close to the MBT. It is considered that the Mahabharat Thrust (MT) (Stocklin 1980) and MCT played the role of sole thrust during emplacement of Lesser Himalayan nappes and crystalline thrust sheets in Nepal Himlaya (Upreti and Le Fort 1999).

GEOLOGY OF HIMALAYAN NAPPES

Numbers of crystalline nappes and thrust sheets (Fig. 1) have been mapped in Nepal Himalaya e.g. from west to east Dadeldhura nappe (Gansser 1964; Bashyal 1986; Upreti 1990), Bajhang nappe (Bashyal 1986; Amatya and Jnawali 1996), Jajarkot nappe (Hagen 1969; Arita et al. 1984) and Kathmandu nappe (Gansser 1964; Hagen 1969; Stocklin 1980). In western Nepal, the Karnali nappe or Chakhure-mabu crystalline klippe are also described (Arita et al. 1984; Hayashi et al. 1984; Kizaki 1994). We briefly describe the geology of the Kathmandu and Karnali nappes because our two simulation models cross sections cut them (for detail see Upreti and Le Fort 1999).

Kathmandu Nappe

The Kathmandu nappe was first recognized by Hagen (1969) and later mapped by Arita et al. (1973), Stocklin and Bhattarai (1977) and Stocklin (1980). The southern part of the Kathmandu nappe almost reaches the MBT and very narrow part of the Lesser Himalayan rocks are sandwitched between crystalline rocks of the Kathmandu nappe and Siwaliks (Fig. 1). The MT separates crystalline rocks of the nappes with underlying Lesser Himalayan autochthonous unit. The MT is considered as a southward continuation of the MCT (Stocklin and Bhattarai 1977; Pandey et al. 1995; Arita et al. 2001; Johnson et al. 2001). Therefore they considered that the HHS and rocks of the Kathmandu nappe are a single tectonic unit, which has thrust over the Lesser Himalaya along the MT. However, recent studies (Rai et al. 1998; Upreti 1999; Upreti and Le Fort 1999; Rai 2001), depending upon the stratigraphy and metamorphism, claimed the existence of two separates nappes; the Gosainkund crystalline nappe in the north and the Kathmandu crystalline nappe in the south separated by MCT placed north of the Kathmandu valley. We consider two separate nappes as considered by Upreti and Le Fort (1999) in this simulation (Fig. 2a).

Kathmandu nappe is composed of the rocks of the Kathmandu Complex, which is divided into Bhimphedi Group and Phulchauki Group (Stocklin 1980). The Bhimphedi Group is the lower unit and is composed of phyllite, schist, metasandstone, quartzite, and marble of Precambrian in age. Small augen gneiss bodies of granitic origin are found in this group. The metamorphic rocks of the Bhimphedi Group are overlain by fossiliferous Lower Paleozoic sequence of the Tethyan affinity belonging to Phulchauki Group. It is composed of limestone, phyllite, calc phyllite, slate and marble. The rocks of the Kathmandu Complex are intruded by several granitic bodies.

The Gosainkund crystalline nappe lies to the north of the Kathmandu valley and consists of amphibolite-granulite facies rocks. It is composed of high-grade metamorphic rocks, which include variety of paragneisses and orthogeisses (augen gneiss, granitic gneiss), mica schist, migmatite, calc silicate gneiss, marble and quartzite.

Karnali Nappe

The Karnali nappe (Karnali klippe of Hayashi et al. 1984) is well exposed along the Karnali and Tila rivers covering area more than 5000 sq. km (Figs. 1 and 2b). Hayashi et al. (1984) carried out the detail geological mapping of this region. This nappe consists of Himalayan gneiss group (equivalent to HHS) and TTS. The crystalline group is divided into garnet biotite kyanite gneiss , calc-siliceous gneiss, augen gneiss and migmatitic gneiss. Near Jumla, the Karnali nappe is separated from Higher Himalayan rocks by only a few km of intervening Lesser Himalayan rocks. Therefore, the root zone of this nappe is very clearly located to HHS (Hayashi et al. 1984; Upreti and Le Fort 1999). TTS consisting of thick piles of carbonates sequence shows the light brick coloured weathering which is typical for Dhaulagiri Limestone of the Tethys Sequence series. The boundary between the Karnali nappe and underlying medium-grade Lesser Himalayan Sequence is marked by thrust (Hayashi et al. 1984).

NUMERICAL SIMULATION

Our purpose of the numerical simulation is to calculate stress distribution and fault development pattern in and around the Himalayan nappes in two-dimensional space. In the present simulation, we assume that rock layers deform elastically until Mohr's stress circle reaches the Mohr-Coulomb failure envelope, after which faulting occurs, the condition can apply for the upper crust. Here, σ_1 and σ_3 are the maximum principal compressive stress and minimum principal compressive stress respectively. Before we present the result of model experiments, we explain model sections, boundary conditions and layer properties used in this modelling.

MODEL SECTIONS

In order to simulate the stress distribution and fault development pattern of the Lesser Himalayan nappes, two

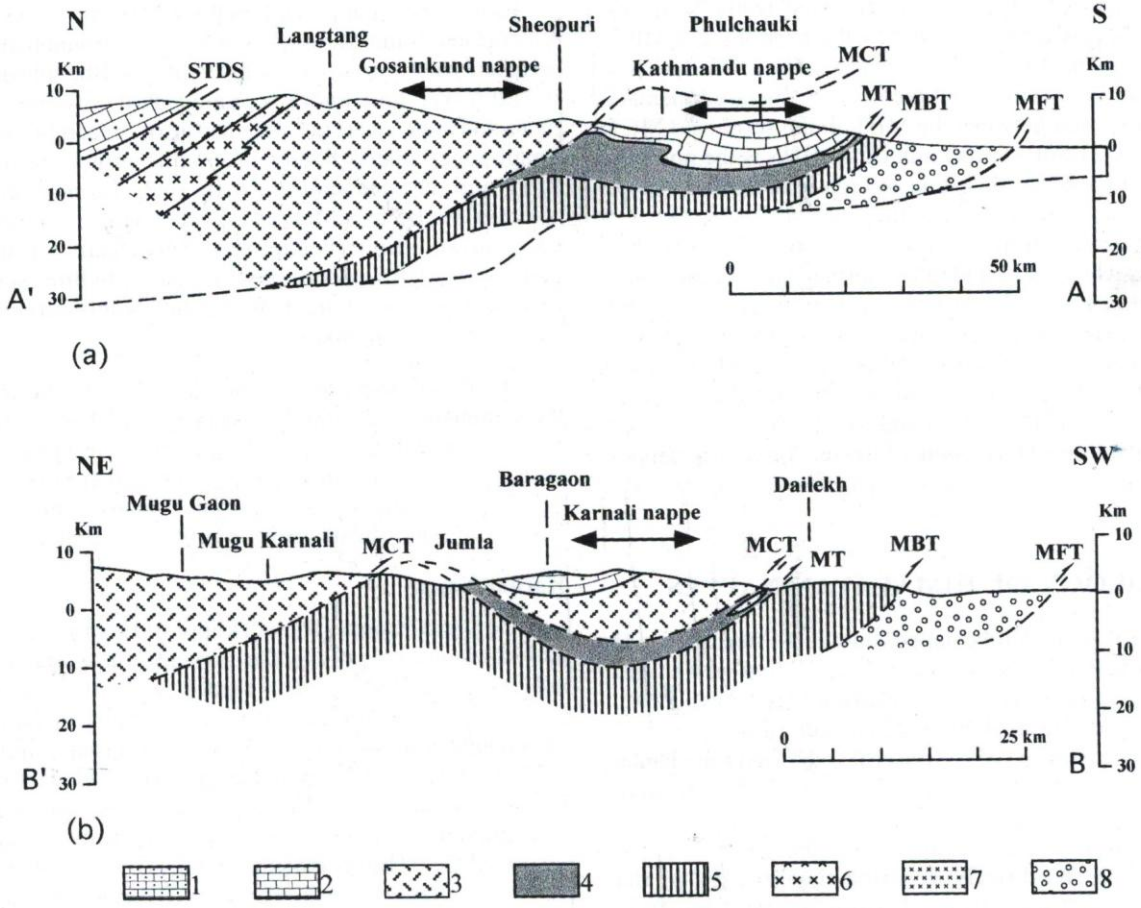

Fig. 2: North-South geological cross sections through the Nepal Himalaya (modified after Upreti and Le Fort 1999). (a) Section through Langtang-Kathmandu along A-A' in Fig. 1. The MCT separates the Gossainkund nappe and the Kathmandu nappe.
(b) Section through western Nepal along B-B' in Fig. 1. The rocks of Karnali nappe show its roots in the Higher Himalayan zones. MFT: Main frontal Thrust, MBT: Main Boundary Thrust, MCT: Main Central Thrust, MT: Mahabharat Thrust, STDS: South Tibetan Detachment System. Legend: 1. Tibetan-Tethys sediments, 2. Phulchauki Group, 3. Higher Himalayan Sequences 4. Bhimphedi Group, 5. Lesser Himalayan rocks, 6. Higher Himalyan leucogranites, 7. Lesser Himalyan granites, 8. Siwalik.

representative cross-sections given by Upreti and Le Fort (1999) have been chosen and are simplified according to available seismotectonic data of central and western Nepal Himalaya (Fig. 2). These cross-sections represent both nappes (Kathmandu and Karnali nappe) of different root zones and lateral variation of geometry of MHT. They also represent zone of high level of seismicity in Nepal Himalaya. The overall length of the model 1 (Kathmandu nappe) is 176 km and thickness varies up to 34 km. Model 2 (Karnali nappe) is about 102 km long and up to 22 km thick.

BOUNDARY CONDITION

Selection of the boundary condition is one of the crucial steps to simulate the tectonic processes. In order to mimic the natural situation, we imposed simple boundary condition representing the present day plate kinematics in the Himalayan fold and thrust belt. In the two section models, the upper surface is free. The lower boundary is only permitted to move horizontally. The nodes along the left boundary of the each model can move vertically only whereas from the right side of the models, we imposed convergent displacement from 50 m (equivalent displacement for 1000 years) at the rate of 5 cm/year (Molnar and Tapponier 1975) to 400 m (equivalent displacement for 8000 years) (Fig. 3).

ROCK LAYER PROPERTIES

For the sake of simplicity in calculation, model 1(Kathmandu nappe) and model 2 (Karnali nappe) were divided into seven and six layers respectively taking enough caution of tectonostratigraphy. Each layer has been assigned

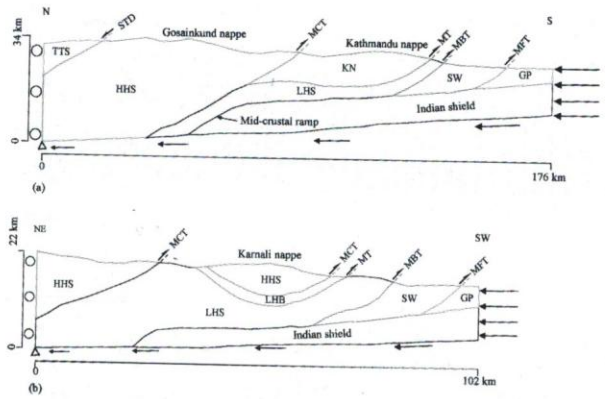

Fig. 3: Geometry and boundary conditions of (a) model (b) model 2.
TTS: Tibetan-Tethys Sediments, HHS: Higher Himalayan Sequence, LH: Lesser Himalaya, LHB: Lesser Himalaya (Bhimphedi Group), SW: Siwalik, GP: Gangetic Plain, STDS: South Tibetan Detachment System, MCT: Main Central Thrust, MT: Mahabharat Thrust, MBT: Main Boundary Thrust, MFT: Main Frontal Thrust.

with distinct rock layer properties giving emphasis on the dominant rock type. We performed series of test calculation using different values of key parameters, viz. density, Young's modulus, Poisson ratio, cohesion and friction angle. We adopted the most suitable set of rock layer properties for calculation, which is shown in Table 1.

MODELLING RESULTS

Stress field around Kathmandu nappe

Stress field under 50m (1000 years) and 400m (8000 years) convergent displacements are shown in Fig. 4 σ_1 and σ_3 show the compressive nature in all part of the models. The magnitude of σ_1 and σ_3 is low in Gangetic Plain, upper part of the Siwalik, Gossainkund nappe, Kathmandu nappe and Tibetan Tethys sequence. This is due to topography and overburden effect. The effect of the ramp on orientation of σ_1 and σ_3 is clear on its upper part where σ_1 rotates from its vertical position. This reveals that the geometry of MHT has significant contributions to the stress orientation in Himalaya. With increasing convergent displacement, the magnitude of σ_1 increases and its axis rotates toward horizontal. Such changes in orientation and magnitude of σ_1 lead to generate thrust faults in the model. This effect is clearly observed in the upper part of each layer except Indian shield (Fig. 4b).

Stress field around Karnali nappe

Stress field under convergent displacement of 50 m (1000 years) and 350 m (7000 years) are shown in Fig. 5. Similar to Model-1 (Kathmandu nappe), stress distribution pattern shows the compressive nature of σ_1 and σ_3. Low magnitude of σ_1 and σ_3 is observed in the upper part of the Higher Himalaya, Lesser Himalaya, Karnali nappe, Siwalik and Gangetic plain. With increasing convergent displacement, the magnitude of σ_1 increases and its orientation becomes horizontal in the upper part of all layers (Fig. 5b). This stress field favors thrust faulting. Similar to Kathmandu nappe model, the axis of σ_1 rotates from vertical position around mid-crustal region. This reveals similar effect (as in Kathmandu nappe) of the geometry of MHT on stress orientation in the western Nepal Himalaya. Moreover, with continued convergence, in the central part of the Indian Shield, north to the junction of MBT/MHT, σ_1 and σ_3 are near the hydrostatic condition, which is due to the effect of boundary condition of the model.

FAILURE ANALYSIS

To observe the fault development pattern in and around the Himalayan nappes, failure analysis was carried out. Mohr-Coulomb criterion was used to find the proximity to

Table 1: Rock layer properties

Layer	Lithology	Density (kg/m^3)	Young's modulus (GPa)	Poisson ratio	Cohesion (MPa)	Friction angle (degree)
IS	Indian Shield, (banded gneiss and granite)	2850	58	0.300	24	52
HHS	Higher Himalayan Sequence (gneiss, granite)	2700	51	0.280	19	47
TTS	Tibetan-Tethys Sequence (limestone)	2660	49	0.270	17	44
KN or LHB	Kathmandu nappe (KN) or LHB (schist, slate, quartzite and limestone)	2620	47	0.230	15	41
LHS	Lesser Himalayan Sequence (phyllite, quartzite and slate)	2400	45	0.195	13	34
SW	Siwalik (mudstone, sandstone and conglomerate)	2320	27	0.180	10	33
GP	Gangetic Plain (Alluvium and Siwalik sediments)	1960	23	0.170	7	31

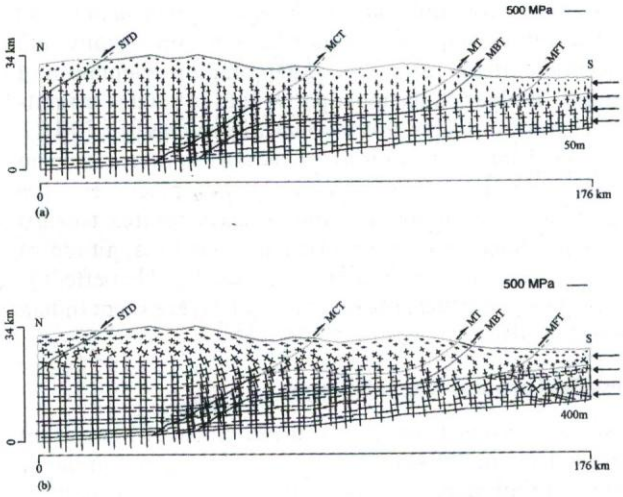

Fig. 4: Stress distribution of model 1.
(a) at 50 m (equivalent for 1000 years) convergent displacement (b) at 400 m (equivalent for 8000 years) convergent displacement. Every pair of perpendicular lines represents σ_1 (long lines) σ_3 (short lines) at each intersection.

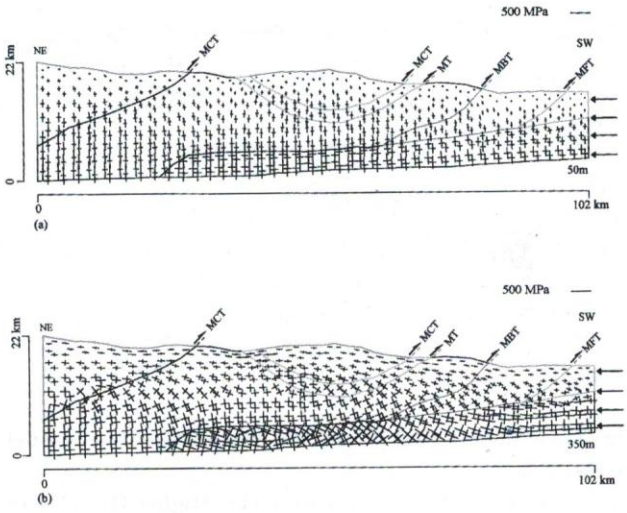

Fig. 5: Stress distribution of model 2.
(a) at 50 m(equivalent for 1000 years) convergent displacement (b) at 350 m(equivalent for 7000 years) convergent displacement. Every pair of perpendicular lines represents σ_1 (long lines) σ_3 (short lines) at each intersection.

rock failure. Although the failure analysis has been described by serial papers (Lu and Hayashi 2001; Alam and Hayashi 2003; Howladar and Hayashi 2003) it is worth for readers to rewrite again hereafter.

Since the analysis is carried out in plane strain condition, it is possible to calculate the value of third principle stress (σ^*), which is perpendicular to σ_1-σ_2 plane using the equation

$$\sigma^* = \nu(\sigma_1 + \sigma_2) \tag{1}$$

where ν is the Poisson ratio (Timosenko and Goodier, 1970; Hayashi and Kizaki, 1972). After comparing the values of σ_1, σ_2 and σ^*, we can recognize the newly defined σ_1, σ_2 and σ_3 as the maximum, intermediate and minimum principal stresses respectively. As shown in Fig. 6, the Mohr-Coulomb criterion is written as a linear relationship between shear and normal stresses,

$$\tau = c + \sigma_n \tan\phi \tag{2}$$

where c and ϕ are the cohesive strength and the angle of internal friction respectively. Failure will observe when the Mohr's circle first touches the failure envelope. It takes place when the radius of the Mohr's circle, $(\sigma_1+\sigma_3)/2$, is equal to the perpendicular distance from the center of the circle at $(\sigma_1-\sigma_3)/2$ to the failure envelope,

$$\left(\frac{\sigma_1-\sigma_3}{2}\right)_{failure} = c\cos\phi + \left(\frac{\sigma_1+\sigma_3}{2}\right)\sin\phi \tag{3}$$

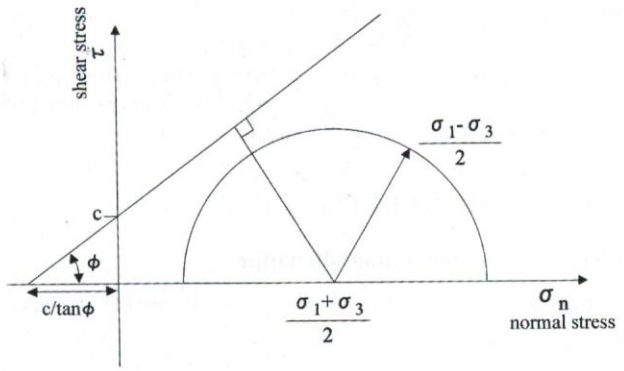

Fig. 6: Mohr-Coloumb criterion

According to Melosh and Williams (1989), the proximity to failure is the ratio between the stress and the failure stress and is given by

$$P_f = \left[\frac{\left(\frac{\sigma_1-\sigma_3}{2}\right)}{\left(\frac{\sigma_1-\sigma_3}{2}\right)_{failure}}\right] \tag{4}$$

When the ratio reaches one (P_f =1), failure occurs, but when $P_f < 1$ stress is within the failure envelope, rock does not fail. The proximity to failure reveals which parts of the model are close to failure or already failed by generating faults.

The type of faulting has been determined by the Anderson's theory (1951). According to his theory three classes of faults (normal, strike slip and thrust) result from the three principal classes of inequality that may exist between the principal stresses.

Fault development around Kathmandu nappe

Simulation shows the development of faults along the base of Gangetic Plain, Siwalik and Lesser Himalayan Sequence (Fig. 7). Under 50 m (1000 years) convergent displacement, normal faulting is dominantly observed around the MBT and MFT. A diffuse zone of failure elements is observed in the LHS, which is located around the mid-crustal ramp. This zone is attributed to the effect of stress accumulation along the mid-crustal ramp and might be related to the microseismic events (Fig. 8a) around the mid crustal ramp shown by Pandey et al. (1999). Further south, normal faults are extensively developed in Siwaliks and the frontal part of MFT. Similar active normal faults associated with major intracrustal thrusts have been recognized in Siwaliks and frontal part of the MFT (equivalent to HFF of Nakata 1982) on the basis of tectonically produced landforms (Nakata 1982, 1989; and Nakata et al. 1984). These active faults generally form a north-dipping imbricated thrust zone in Himalaya (Nakata 1989; Nakata et al. 1990). Thus fault development patterns, predicted by numerical models, show direct correlation with observed geological evidences for active faulting pattern in central Nepal. However, our models do not show any faulting events within the Kathmandu nappe.

Fault development around Karnali nappe

Model 2 (Karnali nappe) shows the similar fault pattern with Model 1 (Kathmandu nappe) under 50 m (1000 years) convergent displacement (Fig. 10a). A elongated zone of failure elements is observed along the northern flat at deeper part of the LHS. The microseismic data of western Nepal Himalaya shows the clustered epicenter distribution in the same locality (Fig. 8b). Therefore this cluster of failure elements might be the cause of microseismic events of the region. Further south normal faults are extensively developed in Siwaliks and Gangetic Plain, which are confined along the major intracrustal thrusts, viz. MBT and MFT. Nakata et al. (1984, 1990) also described similar faulting pattern (Surkhet- Ghorahi Fault) in Dun valleys and frontal part of the MFT (Fig. 9). Similarly, Mugnier et al. (1994) also recognized active steep normal faults close to the MBT in western Nepal Himalaya. With increasing convergent displacement, thrust faults are developed in all part except core of Karnali nappe and its root zone (Fig. 10b). Focal mechanism solution data also show the moderate-magnitude thrust type earthquake beneath the central Himalaya (Seeber et al. 1981; Baranowski et al. 1984; Ni and Barazangi 1984). Thus faulting pattern predicted in this simulation is consistent with the geological evidences.

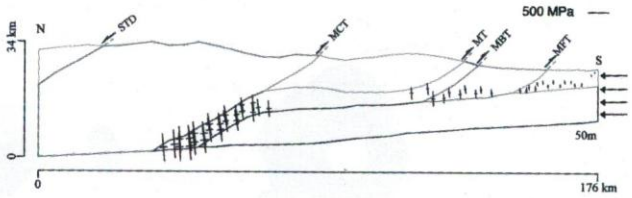

Fig. 7: Failure elements of model 1 at 50 m (equivalent for 1000 years) convergent displacement. Every pair of perpendicular lines represents σ_1 (long lines) σ_3 (short lines) at each intersection.

DISCUSSIONS

Model set-up

The finite element models presented and discussed above, have been performed with two-dimensional space, with a simple geometry of fold an thrust belt assuming homogeneous and isotropic material within the individual layer. In nature the behaviour of rocks is not homogeneous and isotropic. Furthermore, the rock layer properties used in this simulation are not experimentally determined. We performed series of test calculation using different values of key parameters. Finally, we adopted only the most suitable set of layer properties for calculation. However, attention have been paid to avoid wide fluctuation from their real values. We assume that the crust behaves elastically though it is visco-elastic-plastic in nature. Although our models remain simple, assumed data are consistent with known field data.

State of stress in Himalaya

Numbers of authors made attempts to assess the state of stress in the Himalaya and adjacent areas (Cloetingh and Wortel 1986; Shanker et al. 2002,). Nakata et al. (1990) deduced the N-S direction of the maximum horizontal principal stress (σHmax) for eastern and central sectors of the Himalaya using type and strike of the active faults. They further noted that the direction of σHmax have changed following the change in the direction of the relative motion between the Indian plate and the tectonic sliver which have detached together along the transcurrent faults in the Eurasian plate. These studies clearly indicate that regional direction of σHmax is consistent with relative plate motions at least in the central sectors of the Himalaya. We deliberate to set up the model section plane whose strike (approximately NE-SW) coincides with σHmax. Our results show the consistency with the stress state derived from the numerical simulation (Cloetingh and Wortel 1986; Shanker et al. 2002) and active fault studies (Nakata et al. 1990).

Microseismic activity along mid-crustal ramp

Geological, geophysical and structural data have revealed the lateral variation in geometry of the MHT (Zhao

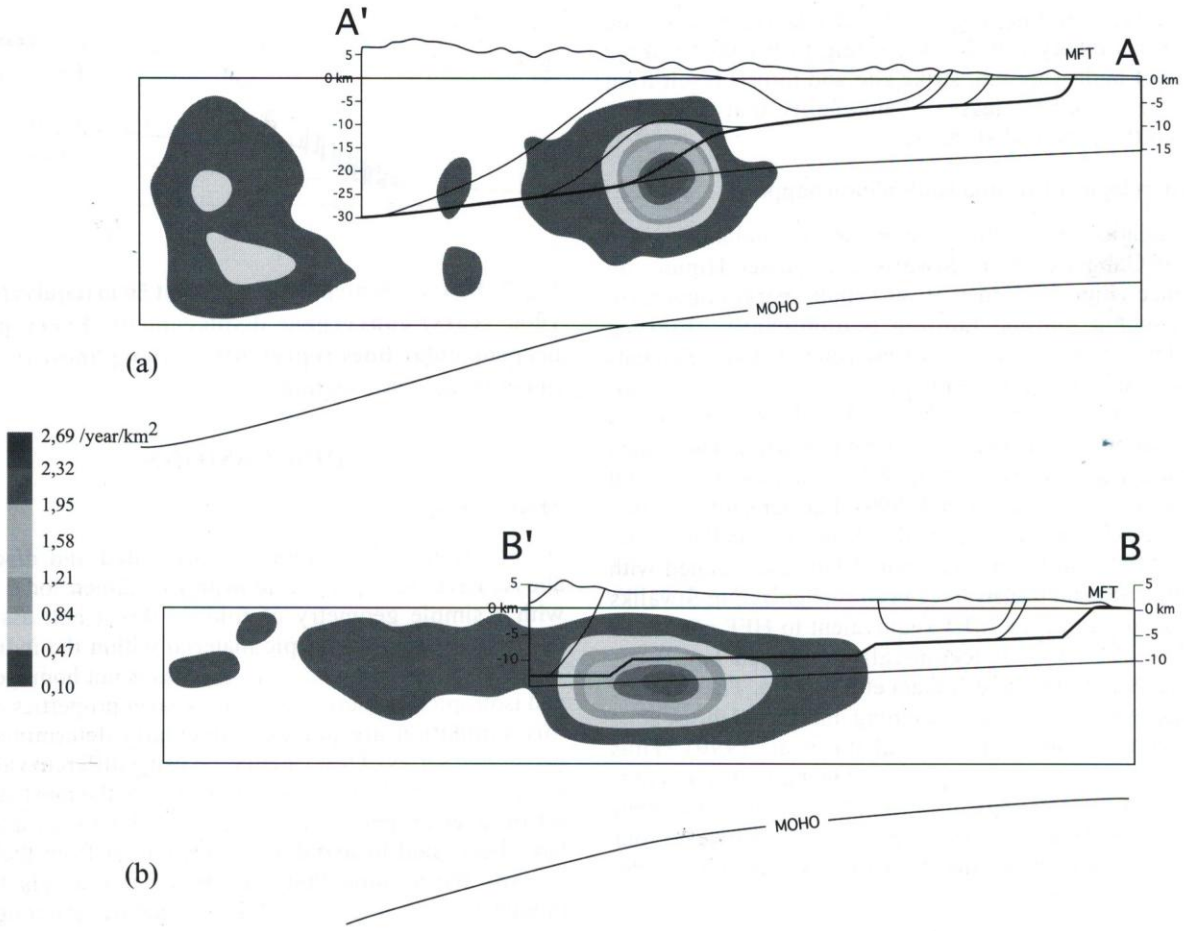

Fig. 8: Density distribution of epicenters (a) central Nepal (b) western Nepal (after Pandey et al. 1999).

et al. 1993; Pandey et al. 1995, 1999). In the central Nepal, structural cross-section shows the existence of decollement at the base of Siwalik sediments, where MFT roots (Schelling and Arita 1991). From the focal mechanism solutions it is proposed that decollement extends beneath the Lesser Himalaya (Baranowski et al. 1984; Ni and Barzangi 1984). This feature is consistent with the MBT flattening out at depth as suggested by Schelling and Arita (1991). Further north, beneath HHS the detachment fault steepens and formed ramp geometry as shown in Fig. 2a. Moreover, additional observations such as variation of terrace height (Iwata et al. 1984) or steepening of the Moho inferred from gravity data (Lyon-Caen and Molnar 1985) also suggest the existence of the active mid-crustal ramp. The mid-crustal ramp, thus, seems to behave as a geometrical asperity where stress is being accumulated during interseismic periods (Pandey et al. 1995). High stress accumulation has been also revealed by geodetic (Jackson et al. 1992) and finite element analysis (Cattin and Avouac 2000; Vergne et al. 2001). This is further supported by clustered microseismic events that follow approximately the topographic front of the Higher Himalaya in central Nepal (Fig. 8a). To the western part of Nepal Himalaya, seismicity map shows two parallel belts that may suggest the existence of two ramps (Pandey et al. 1999). This hypothesis is still to be proved by surface structural data. Similar to central Nepal, microseismic events are also clustered near the ramp flat region in western Nepal beneath the LHS (Fig. 8b). We simulate the realistic stress field and failure elements and are in accordance with the microseismic data of the central and western Nepal Himalayas.

FAULT DEVELOPMENT IN HIMALAYA

Our modelling demonstrates realistic fault patterns in and around the Lesser Himalayan nappes of Nepal Himalaya. We have successfully computed several active faults at their proper location, which conform field observations (Fig. 9). Active faults both normal and thrust types are predicted in Lesser Himalaya, Siwalik and the frontal part of MFT. All models predict faulting to initiate at depth and to transmiting to the surface with increasing convergent displacement and finally propagate towards south. This is consistent with the sequence of thrust development in Himalayan fold and thrust belt. The distribution pattern of faults seems to associate with the major thrusts e.g. MBT and MFT forming north dipping imbricated zone as revealed by field study (Nakata

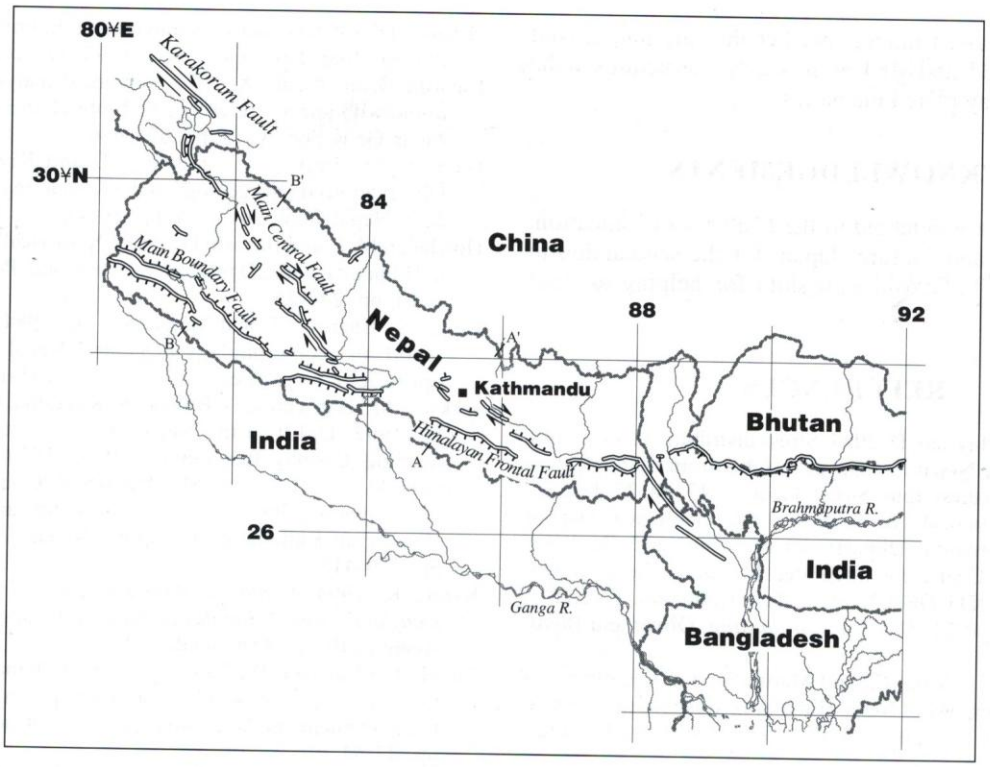

Fig. 9: Active faults in and around Nepal Himalaya. Thick lines without tick marks show newly found active faults. Arrow indicates the direction of strike slip. Down-thrown side is shown by tick marks. A-A' and B-B' show the approximate cross section lines for Fig. 2 (Nakata and Kumahara 2002).

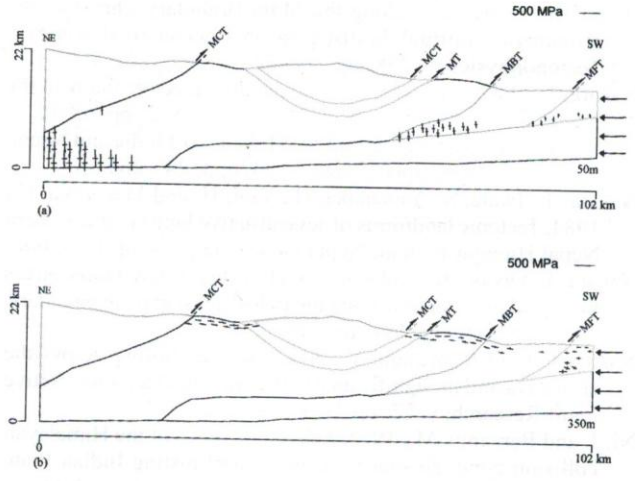

Fig. 10: Failure elements of model 2. (a) at 50 m (equivalent for 1000 years) convergent displacement (b) at 350 m (equivalent for 7000 years) convergent displacement. Every pair of perpendicular lines represents σ_1 (long lines) σ_3 (short lines) at each intersection.

1989). Moreover, we observed faults along the mid-crustal ramp, which shows the active nature of MHT. Thus our models clearly indicate that the mid-crustal ramp, MBT and MFT are the most active structures in the Himalaya.

CONCLUSIONS

Our models allow us to compare state of stress and fault development pattern in the Himalayan fold and thrust belt with field data. Following conclusion can be drawn:

(1) The stress distribution pattern shows the existence of compressive state of stress in the Himalaya.

(2) The magnitude of principal stresses depends upon layer properties and applied convergent displacement. With increasing convergent displacement, the magnitude of increases and its axis rotates towards horizontal resulting thrust fault.

(3) The diffuse zone of failure elements along the mid-crustal ramp and northern flat is attributed to its geometry where stress accumulates during interseimic period.

(4) The fault types, revealed by the simulation suggests the direct correlation with the present day fault development pattern in Himalaya.

(5) The proposed models predict that the mid-crustal ramp, MBT and MFT as most active structures in the present day plate kinematics.

ACKNOWLEDGEMENTS

The authors are indebted to the Ministry of Education, Science, Sports and Culture, Japan, for the scholarship to D.C. We thank Tadayoshi Morishita for helping to draft figures.

REFERENCES

Alam, M.M. and Hayashi, D. 2003, Stress distribution and seismic faulting in the Nepal Himalaya: insights from finite element modeling. Japanese Jour. Struct. Geol., v. 47, pp. 37-48.

Amatya, K. and Jnawali, compillers, 1996, Geological map of Nepal: Kathmandu. Department of Mines and Geology/ International Center for Integrated Mountain Development (DMG/ICMIOD/CDG/UNEP) scale 1:1,000,000. 1 sheet.

Anderson, E., M. 1951, *Dynamics of faulting*. Oliver and Boyd, Edinburg.

Arita, K., Ohta, Y., Akiba, C., and Maruo, Y., 1973, Kathmandu Region. In: Geology of Nepal Himalayas. Hashimoto, S., Ohta, Y., and Akiba, C., (eds.) Tokyo, Saikon Publishing Co. Ltd., 286 p.

Arita, K., Shiraushi, K., and Hayashi, D., 1984, Geology of western Nepal and a comparison with Kumaon, India. Hokkaido University Journal of Faculty of Science, ser., IV, v. 2., pp. 1-20.

Arita, K., Takasu, A., Dhithal, M. R., Regmi, K. R., Hamaguchi, H. and Matsuoka, Y., 2001, Nappe tectonics in the Kathmandu area, central Nepal: single nappe? Or double nappes? Jour. Asian Earth Sci., 16 (3A) 3 (Spec. Abst. Issue. of 16th HKT Workshop).

Baranowski, J., Armbuster, J., Seeber, L., and Molnar P., 1984, Focal depths and fault plane solution of earthquakes and active tectonics of the Himalaya. Jour. Geophy. Res., v. 89, pp. 6918-6928.

Bashyal, R. P., 1986, Geology of Lesser Himalaya, far western Nepal. In Le Fort, P., Colchen, M., and Montenat, C., eds. Evolution des domaines orogeniques d'Asie meridionale (de la Turquie a l'Indonesie): Nancy, France, Sciences de la terre. Memoire, v. 47, pp. 31-42.

Burchfiel, B.C., Zhiliang, C., Hodges, K. V., Yuping, L., Royden, L. H., Changrong, D., and Jiene, X., 1992, The south Tibetan detachment system, Himalayan orogen: Extension contemporaneous with and parallel to shortening in a collisional mountain belt. Geol. Soc. Ame., v. 269, pp. 1-41.

Cattin, R. and Avouac, J. P., 2000, Modelling mountain building and the seismic cycle in the Himalaya of Nepal. Jour. Geophy. Res., v. 105, B6, pp. 13389-13407.

Cloetingh, S. and Wortel, R., 1986, Stress in the Indo-Australian Plate. Tectonophysics, v. 132, pp. 49-67.

England, P. and McKenzie, D., 1982, A thin viscous sheet model for continental deformation. Geophy. Jour. Astr. Soc., v. 70, pp. 295-321.

Gansser. A., 1964, *Geology of the Himalayas*. London, Interscience Publishers, John Wiley and Sons, 289 p.

Hagen,T., 1969, Report on the geological Survey of Nepal, Volume 1. Preliminary reconnaissance: Zurich. Denkschriften der Schweizerischen Naturforschenden Gesellshaft, Memories de la Societe Helcetique des Science, 86, 185 p.

Hayashi, D., 1987, Numerical simulation of the uplift of the Tibetan Plateau. Jour. Japan Geol. Soc., v. 93 (8), pp. 587-595.

Hayashi, D. and Kizaki, K, 1972, Numerical analysis on migmatite dome with special reference to finite element method. Jour. Japan Geol. Soc., v. 78, pp. 677-686.

Hayashi, D., Fujii, Y., Yoneshiro, T. and Kizaki, K., 1984, Observations on the geology of the Karnali region, west Nepal. Jour. Nepal Geol. Soc., v. 4, pp. 29-40.

Howladar, M. F. and Hayashi D., 2003, Numerical fault simulation in Himalayas with 2D finite element method. Polar Geoscience, v. 16, pp. 244-258.

Iwata, S., Sharma, T. and Yamanaka, H., 1984, A preliminary report on geomorphology of central Nepal and Himalayan uplift. Jour. Nepal Geol. Soc., v. 4, pp. 141-149.

Jackson, M.; Barrientos, S.; Bilham, R. Kayestha, D. and Shrestha, B., 1992, Uplift in the Nepal Himalaya revealed by sprit leveling. Geophy. Res. Lett., v. 19, pp. 1539-1542.

Johnson, M.R.W., Oliver, G.J.H., Parrish, R.R. and Johnson, S.P., 2001, Synthrusting metamorphism, cooling and erosion of the Himalayan Kathmandu Complex, Nepal. Tectonics, v. 20, pp. 394-415.

Kizaki, K., 1994, *An outline of the Himalayan Upheaval: A case study of the Nepal Himalayas*. Japan International Cooperation Agency (JICA), Kathmandu. 127 p.

Lu, H. and Hayashi, D., 2001, Genesis of Okinawa Trough and thrust development within accretionry prism by means of 2D finite element method. Japanese Jour. Struct. Geol., v. 45, pp. 47-64.

Lyon-Caen, H. and Molnar P., 1985, Gravity anamoliies, flexure of the Indian plate and the suture, support and evolution of the Himalaya and Ganga basin. Tectonics, v. 4, pp. 513-538.

Melosh, H. J. and Williams, JC.A., Jr, 1989, Mechanics of graben formation in crustal rocks: A finite element analysis, Jour. Geophy. Res., v. 94, pp. 13961-13973.

Molnar, P. and Tapponier, P., 1975, Cenozoic tectonics of Asia: effect of a continental collision. Science, v. 189, pp. 419-426.

Mugnier, J.-L., Huyghe, P., Chalaron, E. and Mascle, G. 1994, Recent movements along the Main Boundary Thrust of the Himalayas: normal faulting in an over-critical wedge?, Tectonophysics, v. 238, pp. 199-215.

Nakata, T., 1982, A photogrammetric study on active faults in the Nepal Himalayas. Jour. Nepal Geol. Soc., v. 2, pp. 67-80.

Nakata, T., 1989, Active faults of the Himalaya of India and Nepal. Geol. Soc. Ame., Spec. Paper, v. 232, pp. 243-263.

Nakata, T., Iwata, S., Yamanaka, H., Yagi, H. and Maemoku, H., 1984, Tectonic landforms of several active faults in the western Nepal Himalayas. Jour. Nepal Geol. Soc., v. 4, pp.177-200.

Nakata, T., Otsuki, K., and Khan, S. H., 1990, Active faults, stress field, and plate motion along the Indo-Eurasian plate boundary. Tectonophysics, v. 181, pp. 83-95.

Nakata, T. and Kumahara, Y., 2002, Active faulting across the Himalaya and its significance in the collision tectonics. Active Fault Research, v. 22, pp.7-16.

Ni, J. and Barzangi, M., 1984, Seismotectonics of the Himalayan collision zone: geometry of the underthrusting Indian Plate beneath the Himalaya, Jour. Geophys. Res. v. 3, pp.1-11.

Pandey, M. R., Tandukar, R. P., Avouac J. P., Lave J., and Massot, J. P., 1995, Interseismic strain accumulation on the Himalayan crustal ramp (Nepal). Geophys. Res. Lett., v. 22, pp. 751-754.

Pandey, M. R.,Tandukar, R. P., Avouac, J. P., Vergne, J., and Heritier, 1999, Seismotectonics of the Nepal Himalaya from a local seismic network. Jour. Asian Earth Sci., v. 17, pp. 703-712.

Patrait, P. and Achache, J., 1984, India-Eurasia collision chronology and its implications for crustal shortening and driving mechanisms of plates. Nature, v. 311, pp. 615-621.

Rai, S. M., 2001, Geology, geochemistry, and radiochronology of the Kathmandu and Gosainkund cryastalline nappes, central Nepal Himalaya. Jour. Nepal Geol. Soc., v. 25, pp. 135-155.

Rai, S. M., Guillot, S., Le Fort, P. and Upreti, B. N., 1998, Pressure temperature evolution in the Kathmandu and Gosainkund region, central Nepal. Jour. Asian Earth Sci., v. 16, pp. 283-298.

Schelling, D. and Arita, K., 1991, Thrust tectonics, crustal shortening and the structure of the far eastern Nepal Himalaya. Tectonics, v. 10, pp. 851-862.

Seeber, L., Armbruster, J. G., and Quittmeyer, R. C., 1981, Seismicity and continental subduction in the Himalayan arc. Geodynamics Serie, v. 3, pp. 215-242.

Shanker, D., Kapur, N. and Singh, B., 2002, Thrust-wedge mechanics and coeval development of normal and reverse faults in the Himalayas. Jour. Geol. Soc., London, v. 159, pp. 273-280.

Stocklin, J., 1980, Geology of the Nepal and its regional frame. Jour. Geol. Soc. London, v. 137, pp. 1-34.

Stocklin, J. and Bhattarai, K.D., 1977, Geology of Kathmandu area and central Mahabharat Range, Nepal Himalaya. HMG Nepal/UNDP report, 64 p.

Thakur, V. C., 2001, Regional geology and geological evolution of the Himalaya, in Landslide Hazard Mitigation in the Hindu Kush- Himalayas (Eds. Li Tianchi, Suresh Raj Chalise and Bishal Nath Upreti) ICIMOD, Kathmandu, pp. 3-15.

Timoshenko, S. P. and Goodier, J. N., 1970, *Theory of elasticity.* McGraw-Hill, London, International edition, 567 p.

Upreti, B., N., 1990. An outline of geology of far western Nepal. Jour. Him. Geol., v.1, pp. 93-102.

Upreti, B.N., 1999, An overview of the stratigraphy and tectonics of the Nepal Himalaya. Jour. Asian Earth Sci., 17, pp. 577-606.

Upreti, B. N. and Le Fort, P., 1999, Lesser Himalayan crystalline nappes of Nepal: problem of their origin. In: Macfarlane, A., Quade, J., Sorkhabi , R., Eds.), Geol. Soc. Ame. Spec. Paper, v. 328, pp. 225-238.

Vergne, J., Cattin, R., and Avouac, J. P., 2001, On the use of dislocations to model interseismic strain and stress build-up at the intracontinental thrust faults. Geophys. Jour. Int., v. 47, pp. 155-162.

Zhao, W., Nelson, K. D., and Project INDEPTH Team, 1993, Deep seismic reflection evidence for continental underthrusting beneath southern Tibet. Nature, v. 366, pp. 557-559.